Pulsed quantum cascade laser based hypertemporal real-time headspace measurements

Toby K. Boyson,[1] Dylan R. Rittman,[2] Thomas G. Spence,[3] Maria E. Calzada,[3] Abhijit G. Kallapur,[1] Ian R. Petersen,[1] K. Paul Kirkbride,[4] David S. Moore, [2] and Charles C. Harb[1,*]

[1] *School of Engineering and Information Technology, UNSW Australia, Canberra, ACT 2600, Australia*

[2] *Shock and Detonation Physics Group, Los Alamos National Laboratory, Los Alamos, NM 87545, USA*

[3] *Department of Chemistry, Loyola University New Orleans, New Orleans, LA 70118, USA*

[4] *School of Chemical and Physical Sciences, Flinders University, Adelaide, SA, 5001, Australia*

c.harb@adfa.edu.au

Abstract: Optical cavity enhancement is a highly desirable process to make sensitive direct-absorption spectroscopic measurements of unknown substances, such as explosives, illicit material, or other species of interest. This paper reports advancements in the development of real-time cavity ringdown spectroscopy over a wide-bandwidth, with the aim to make headspace measurements of molecules at trace levels. We report results of two pulsed quantum cascade systems operating between (1200 to 1320)cm^{-1} and (1316 to 1613)cm^{-1} that measure the headspace of nitromethane, acetonitrile, acetone, and nitroglycerin, where the spectra are obtained in less than four seconds and contain at least 150,000 spectral wavelength datapoints.

© 2014 Optical Society of America

OCIS codes: (120.6200) Spectrometers and spectroscopic instrumentation; (300.1030) Absorption; (300.6340) Spectroscopy, infrared; (300.6360) Spectroscopy, laser.

References and links

1. D.S. Moore, "Recent advances in trace explosives detection instrumentation," Sens. Imag. **8**, 9-38 (2007).
2. J.S. Caygill, F. Davis, and S.P.J. Higson, "Current trends in explosives detection techniques," Talanta **88**, 14-29 (2012).
3. R.G. Ewing, D.A. Atkinson, G.A. Eiceman, and G.J. Ewing, "A critical review of ion mobility spectrometry for the detection of explosives and explosive related compounds," Talanta **54**(3), 515-529 (2001).
4. I.Gazit, J.Terkel, "Explosives detection by sniffer dogs following strenuous physical activity," Appl. Anim. Behav. Sci. **81**(2), 149-161 (2003).
5. T.G. Spence, C.C. Harb, B.A. Paldus, R.N. Zare, B. Wilke, and R.L. Byer, "A laser-locked cavity ring-down spectrometer employing an analog detection scheme," Rev. Sci. Instrum. **71**(2), 347-353 (2000).
6. T.K. Boyson, T.G. Spence, M.E. Calzada, and C.C. Harb, "Frequency domain analysis for laser-locked cavity ringdown spectroscopy," Opt. Express **19**(9), 8092-8101 (2011).
7. J.Ye, L. Ma, and J.L. Hall, "Ultrasensitive detections in atomic and molecular physics: demonstration in molecular overtone spectroscopy," J. Opt. Soc. Am. B: Opt. Phys. **15**(1), 6-15 (1998).
8. T.G. Spence, M.E. Calzada, H.M. Gardner, E. Leefe, H.B. Fontenot, L. Gilevicius, R.W. Hartsock, T.K. Boyson, and C.C. Harb, "Real-time FPGA data collection of pulsed-laser cavity ringdown signals," Opt. Express **20**(8), 8804-8814 (2012).

#205644 - $15.00 USD Received 28 Jan 2014; revised 16 Mar 2014; accepted 26 Mar 2014; published 24 Apr 2014

9. C. Ramos, P.J. Dagdigian, "Detection of vapors of explosives and explosive-related compounds by ultraviolet cavity ringdown spectroscopy," Appl. Opt. **46**(4), 620-627 (2007).
10. A.D. Usachev, T.S. Miller, J.P. Singh, F. Yueh, P. Jang, and D.L. Monts, "Optical properties of gaseous 2,4,6-trinitrotoluene in the ultraviolet region," Appl. Spectrosc. **55**(2), 125-129 (2001).
11. C. Ramos, P.J. Dagdigian, "Effect of photochemistry on molecular detection by cavity ringdown spectroscopy: case study of an explosive-related compound," Appl. Opt. **46**(26), 6526-6532 (2007).
12. M. Snels, T. Venezi, and L. Belfiore, "Detection and identification of TNT, 2,4-DNT and 2,6-DNT by near-infrared cavity ringdown spectroscopy," Chem. Phys. Lett. **489**, 134-140 (2010).
13. M.W. Todd, R.A. Provencal, T.G. Owano, B.A. Paldus, A. Kachanov, K.L. Vodopyanov, M. Hunter, S.L. Coy, J.I. Steinfeld, and J.T. Arnold, "Application of mid-infrared cavity-ringdown spectroscopy to trace explosives vapour detection using a broadly tunable optical parametric oscillator," Appl. Phys. B **75**, 367-376 (2002).
14. C.C. Harb, T.K. Boyson, A.G. Kallapur, I.R. Petersen, M.E. Calzada, T.G. Spence, K.P. Kirkbride, and D.S. Moore, "Pulsed quantum cascade laser-based CRDS substance detection: real-time detection of TNT," Opt. Express **20**(14), 15489-15502 (2012).
15. M.J. Thorpe, K.D. Moll, R.J. Jones, B. Safdi, and J. Ye, "Broadband cavity ringdown spectroscopy for sensitive and rapid molecular detection," Science **311**(5767), 1595-1599 (2006).
16. B. Bernhardt, A. Ozawa, P. Jacquet, M. Jacquey, Y. Kobayashi, T. Udem, R. Holzwarth, G. Guelachvili, T.W. Haensch, and N. Picque, "Cavity-enhanced dual-comb spectroscopy," Nat. Photonics **4**(1), 55-57 (2009).
17. C.G. Tarsitano, and C.R. Webster, "Multilaser Herriott cell for planetary tunable laser spectrometers," Appl. Opt. **46**(28), 6923-6935 (2007).
18. M.S. Taubman, T.L. Myers, B.E. Bernacki, R.D. Stahl, B.D. Cannon, J.T. Schiffern, and M.C. Phillips, "A modular architecture for multi-channel external cavity quantum cascade laser-based chemical sensors: a systems approach," Proc. of SPIE **8268**, 82682G (2012).
19. P. Zalicki, R.N. Zare, "Cavity ring-down spectroscopy for quantitative absorption measurements," J. Chem. Phys. **102**, 2708 (1995).
20. J.J. Harrison, N Humpage, N.D.C. Allena, A.M. Waterfall, P.F. Bernath, and J.J. Remedios, "Mid-infrared absorption cross sections for acetone (propanone)," J. Quant. Spectrosc. Radiat. Transfer **112**(3), 457-464 (2011).
21. R.G. Smith, N. D'Souza, and S. Nicklin, "A review of biosensors and biologically-inspired systems for explosives detection," Analyst **133**(5), 571-584 (2008).
22. O. Leitch, O, A. Anderson, K.P. Kirkbride, and C. Lennard, "Biological organisms as volatile compound detectors: A review," Forensic Sci. Int. **232**(1-3), 92-103 (2013).

1. Introduction

Real-time headspace analyzers are highly desirable for the rapid measurement of hostile environments [1, 2]. Ion mobility spectrometers [3], for example, are commonly used as a screening instrument due to their sensitivity and rapid analysis time, but struggle with selectivity. Dogs are still used heavily as headspace detectors, but they are not able to unequivocally state what chemicals are present, and in what concentration. Moreover, as would be expected from any animal, dogs get tired, they require regular "refresher" training, and have at least some degree of variability in their response to stimuli amongst different animals, and even with the same animal on different occasions [4]. In extremely hostile environments, such as a fire or industrial accident, responders struggle to find instruments that can quickly analyze the hazards, and sending in dogs would be ill-advised.

Spectroscopic techniques have the potential to offer the best combination of sensitivity, selectivity, and speed, and are non-destructive (unlike mass spectrometers, MS). Moreover, in the hands of expert users or with the aid of spectral libraries, wide-band spectroscopic data can be used to identify non-target compounds that are present. Sensitive, indirect techniques such as laser induced fluorescence (LIF) and photoacoustic spectroscopy (PAS) have been applied to explosives detection, but they suffer from an inability to detect non-fluorescing species (for example, triacetone triperoxide (TATP)) and a sensitivity to atmospheric noise, respectively. Broadband direct absorption techniques (such as Fourier Transform infrared spectroscopy (FTIR)) offer rapid analysis times and broad spectral bandwidths, but tend to not have the spectral resolution, or be sensitive enough. Very sensitive, high resolution techniques, such as locked CRDS instruments [5, 6] or Noise Immune Cavity Enhanced Optical Heterodyne Molecular Spectroscopy (NICE-OHMS) [7], tend to offer low spectral bandwidths, restrict-

#205644 - $15.00 USD Received 28 Jan 2014; revised 16 Mar 2014; accepted 26 Mar 2014; published 24 Apr 2014
(C) 2014 OSA

ing their ability to distinguish absorption features of interest from interfering absorptions and to identify unknown or unexpected analytes. Moreover, these techniques rely on complicated experimental setups that are ill suited to use outside of a laboratory. The broader the tuning range, the more information is gathered, and thus a wider range of explosives can be detected and greater is the potential there is to discriminate explosives from innocent substances such as nitromusks present in perfumes and personal care products: this is especially relevant to large, nitro- containing species, whose spectra tend to have broad peaks, rather than the narrow, rotationally resolved peaks studied with conventional narrow-band CRDS instruments.

Cavity ringdown spectroscopy is a technique that, rather than measuring relative attenuation after a light source passes through a sample, measures the temporal decay of a light field within an optical cavity. The benefits here are twofold: the cavity provides a long effective pathlength (several kilometers being common); and the measurement of a decay constant rather than intensity decouples the measurement from laser intensity noise. This means that even noisy, pulsed lasers are able to be used to acquire spectra with high sensitivity [8]. Ramos [9] and Usachev [10] used CRDS in the UV to study vapor phase DNT and TNT: while the instrument was sensitive (due to the high absorption cross sections for the nitro group in that wavelength range), the low tunability and the broadness of spectral features in UV would make it difficult to unambiguously assign spectral features to a compound, even without the presence of masking or interfering species. The same authors [11] report that the UV light can cause the molecules inside the cavity to dissociate and breakdown: this would further complicate the narrow spectral bandwidth spectra. Snels [12] used CRDS in the near infrared (NIR), scanning across 100 nm with a centre wavelength of 1550 nm. While they report detection limits on the order of nanograms for TNT and DNT, their implementation resulted in only being able to acquire 33 ringdown events per second: this resulted in it taking tens of seconds to acquire a single spectrum, and several minutes to acquire an adequate signal-to-noise for unambiguous identification of the compound. Moreover, they only scan across a single absorption feature (probably due to the tuning range of the external cavity diode laser used in the work): this would make it challenging to unambiguously identify a given compound. The area that shows the most promise for the detection is the mid infrared (MIR): Todd *et al.* [13], using a pulsed optical parametric oscillator (OPO) took spectra for several common explosives from 7-8 μm. The repetition rate of their laser was 25 Hz: this limited the rate at which spectra could be acquired, with Todd noting that a practical implementation of the instrument would only monitor several wavelengths, rather than the entire spectrum. While this would increase the throughput of their technique, it would limit the ability to resolve peaks in the presence of interfering absorptions. Clearly, a better approach would be to increase the rate at which the instrument could acquire and analyze data: ideally, the technique should be limited by the scan rate of the laser, and not by the time taken to process the data.

We report here on a variant of Pulsed CRDS that is able to acquire more than 150,000 spectral datapoints in less than four seconds, while scanning across more than 1400 nm ($\approx 300 cm^{-1}$) in the mid infrared. Most CRDS experiments treat the analysis of ringdown data as a time-domain problem: some method is used to build up light in the cavity, then, when the light has reached a predetermined level, the light is shuttered and the exponential decay of the cavity is measured. This decay is typically fit with a non-linear least squares fitting algorithm: this scheme is appropriate for a slow pulsed instrument, but for faster throughputs, the fitting fails to keep up with the rate of data collection (in our experience, by up to two orders of magnitude [8, 6]).

There is, through the Fourier transform, a frequency domain approach. The cavity acts as a low pass filter (with a corner frequency of $1/\tau$ rad/sec) with respect to any modulation on the incident light, giving an alternative view of CRDS: rather than thinking about τ decreasing as a

#205644 - $15.00 USD Received 28 Jan 2014; revised 16 Mar 2014; accepted 26 Mar 2014; published 24 Apr 2014
(C) 2014 OSA

function of absorption within the cavity, we can think about the corner frequency of a low pass filter moving to a higher frequency as the absorption inside the cavity increases. By exciting the cavity with amplitude modulated light (in this work, a pulse train, but we have shown the technique to be applicable to squarewave modulated light as well [6, 8, 14]) and measuring the relative attenuation the harmonic components, τ can be calculated. For the case here, where we are using a pulse train, and measuring the ratio of the second harmonic to the fundamental, τ is given by:

$$\tau = \frac{1}{\omega}\sqrt{\frac{1-P}{4P-1}} \tag{1}$$

Where P is the magnitude of the ratio of the second harmonic to the fundamental, and ω is the pulse angular frequency in rad/s. This methodology has several advantages over a traditional time-domain fitting algorithm: the detection wavelength bandwidth is very large, while maintaing high wavelength resolution; we are able obtain and analyze data as it arrives from the spectrometer, rather than having to acquire a ringdown and batch process; and, as we are measuring the ratio of frequency harmonic components, we maintain the insensitivity to laser amplitude fluctuations that is an important attribute of a cavity ringdown measurement.

2. Real-time headspace measurements

2.1. Optical system

The spectrometer design used in this research was chosen for its simplicity and robustness, with a view to the development of a rugged and small spectrometer. This system is complementary to that described in other cavity enhanced techniques such as [15, 16] that offer excellent sensitivities and broad tuning range. It also differs from the multipass techniques such as [17, 18] by being on axis with the cavity eigenmode, and hence less susceptible to coating irregularities at the mirror edges. A simplified diagram of the instrument is shown in Fig. 1. It consists of a broadly tuning external cavity Quantum Cascade Laser (QCL) from Daylight Solutions Inc. (Model ÜT-7 set to pulse frequency 130 kHz and pulse width 500 ns, the manufacturer specified pulse width is $< 1\ cm^{-1}$, the laser's wavelength was scanned using the inbuilt external grating) , mode matching optics (MMO) consisting of a pair of CaF_2 plano-convex lenses (the beam from the laser passes through a 100 mm lens then a 250 mm lens to match the QCL waist to that of the cavity), an optical cavity (fitted with three $R = 99.9\%$ mirrors and one $R = 99.8\%$ mirror (radius of curvature 1 meter) supplied by LohnStar Optics Inc.,), giving an empty cavity ringdown time of the order of 1 μs, or, equivalently, a cavity corner frequency of 160 kHz, a mercury-cadmium-telluride (MCT) detector from Kolmar Inc. (KMPV8-1-J1/DC, 50 MHz bandwidth, operated at 40 mV signal output here, and 2 V output later in the paper), and a pair of lock-in amplifiers (Stanford Research Systems SR844, both set to 100 μs time constant and 20 $dB/decade$ roll off) configured to measure the in phase and quadrature components of the fundamental and the second harmonic of the pulse train after it passes through the cavity. The data from the lock-in amplifiers were digitised using a National Instruments 100 kS/s data acquisition card, and processed in Labview, or exported and post-processed in Matlab. The optical system was chosen to be a 4 mirror ring shape (2 meter single pass optical, corresponding to a free spectral range of 150 MHz) pathlength to ensure that back reflections to the laser were minimized without the need of an optical isolator. With approximately 2.5 mW (time averaged) of light incident on the cavity, there was approximately 1 μW incident on the detector, corresponding to a peak voltage of approximately 40 mV. The wavelength reading was taken directly off of the laser's display.

#205644 - $15.00 USD Received 28 Jan 2014; revised 16 Mar 2014; accepted 26 Mar 2014; published 24 Apr 2014
(C) 2014 OSA

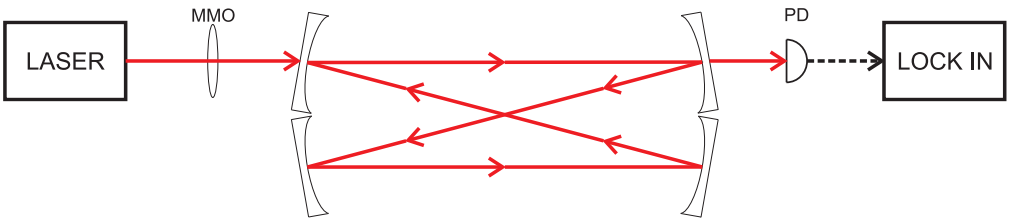

Fig. 1. Schematic of the real-time CRDS experiment. LASER: external cavity MIR QCL; MMO: mode matching optics; PD: liquid nitrogen cooled MCT photodetector; LOCK IN: 2 lock-in amplifiers. Optical paths are shown in red; electrical in dashed black.

The mirrors were held in on an aluminum spacer (machined such that the mirrors were angled correctly to form a stable optical resonator) using a backing plate that could be bolted directly to the end faces. Rubber o-rings were sandwiched between the spacer and mirror surfaces, and hence acted as vacuum seals for the cell. Note that, no tuning elements such as piezoelectric ceramics were used and the system was not actively cooled or heated. The cavity was evacuated using a turbomolecular pump to $\approx 10^{-4}$ *Pa*.

The external cavity QCL was operated at a maximum scan rate of 100 cm^{-1}/s, but in general the scan rate was chosen to ensure that adequate time was allowed for the cavity buildup and ringdown to occur at least twice before changed wavelengths. In the optical system described here, we chose to scan the tuning range at $\approx 75 cm^{-1}/s$.

2.2. Sensitivity and species identification measurements: (1316 to 1613)cm^{-1} system.

Figure 2 shows the transmitted signal power, as measured by the lock-in amplifiers, at the fundamental laser pulse frequency and the second harmonic after the laser beam has travelled from the QCL source to the cavity, through the evacuated cavity, and to the detector. The figure shows that the power of the laser light is greatly attenuated at many wavelengths as it travels the almost 1m distance from QCL to detector. The power ratio, on the other hand, is extremely smooth and shows little variation in spite of the large laser power changes. This is due to the fact that the power changes for the fundamental and second harmonic are highly correlated for changes that occur outside the CRDS cavity, and hence their ratio remains constant.

In order to quantify the noise equivalent absorbance of our instrument and technique, we have used the methodology of Zalicki and Zare [19]. The minimum detectable absorption loss (MDAL) is expressed in terms of the minimum detectable loss per cm along the optical path length with a hypothetical one second of averaging time (*i.e.*, units of $cm^{-1}/\sqrt{Hz}$). The best result for a CRDS experiment, $\approx 10^{-12}$ $cm^{-1}/\sqrt{Hz}$ was published by Spence *et al.* [5], but this was a complicated experiment that was only able to scan across several nanometers. More typical pulsed CRDS experiments achieve MDALs of the order of $\approx 10^{-9}$ $cm^{-1}/\sqrt{Hz}$. The MDAL is calculated from:

$$MDAL_{raw} = \frac{1}{c}\left(\frac{1}{\tau - \Delta\tau} - \frac{1}{\tau}\right) \tag{2}$$

Where $\Delta\tau$ is some measure of the standard deviation for a given measurement set (here, it is the 2σ deviation), c is the speed of light (in cm/s). $MDAL_{raw}$ is in units of cm^{-1}: this is normalised by the square root of the time taken to acquire a spectral datapoint to give the *MDAL* in $cm^{-1}/\sqrt{Hz}$. To calculate the MDAL, we have generated a background spectrum (shown in Fig. 3), fitted it with a polynomial, and then calculated a standard deviation from the residuals (shown in Fig. 3). For these data, the standard deviation is $\approx 1.2 \times 10^{-8}$ seconds. Given a mean τ of 7.8×10^{-7} seconds, and assuming a sweep time (time taken to scan across the wavelength

#205644 - $15.00 USD Received 28 Jan 2014; revised 16 Mar 2014; accepted 26 Mar 2014; published 24 Apr 2014
(C) 2014 OSA

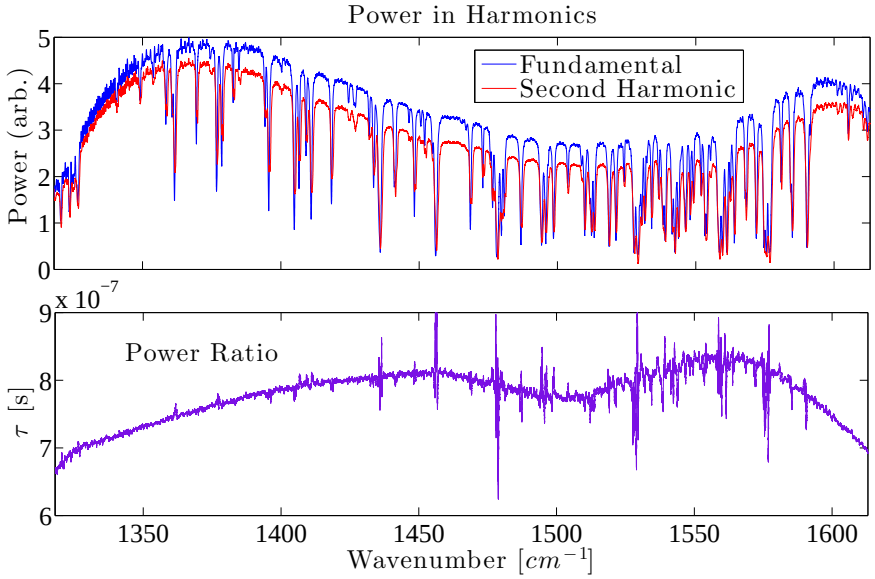

Fig. 2. Transmission spectrum the QCL signal as it travels over 1m of room air. Shown are the fundamental and second harmonic signals after 1m of travel compared to the derived τ from the ratio of the two powers. There is a slight time offset between the two lock-in amplifiers, resulting in the large spikes seen in the lower figure. We have corrected this problem by using a single lock-in amplifier and improving the laser's coupling to the cavity, as discussed later in the paper.

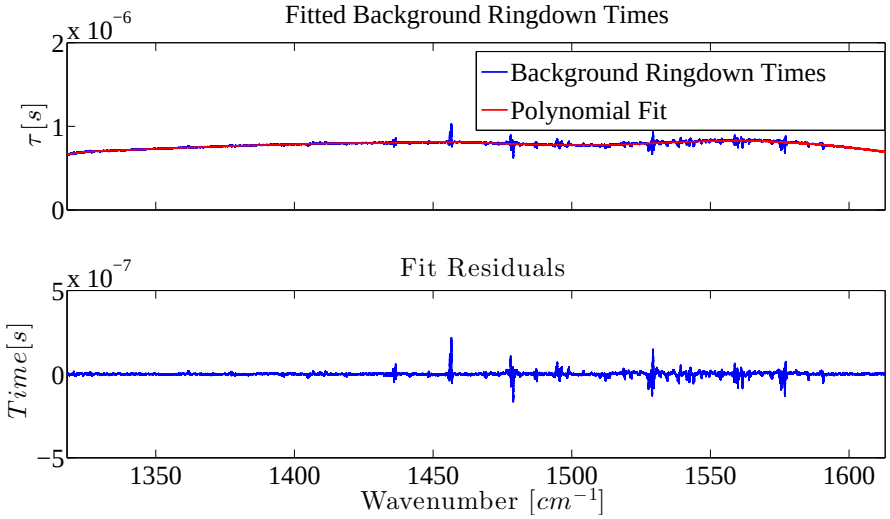

Fig. 3. Polynomial fit to background, and residuals. As noted in Fig. 2, the spikes in the background signal are caused by a time offset between the two lock-in amplifiers.

#205644 - $15.00 USD Received 28 Jan 2014; revised 16 Mar 2014; accepted 26 Mar 2014; published 24 Apr 2014
(C) 2014 OSA

range) of 3.8 seconds, and noting that the background is the average of 6 sweeps (this results in a time-per-point of $\left(\frac{3.8}{152{,}000} \times 6\right)$ *seconds*), this gives a MDAL of $8.1 \times 10^{-9}\ cm^{-1}/\sqrt{Hz}$.

Given these MDALs, we can calculate detection limits for acetone and nitromethane. Given the absorption cross section of $\approx 3 \times 10^{-19}\ cm^2/molecule$ in this wavelength for acetone [20], we calculate the minimum detectable concentration as $1.03 \times 10^{-9}\ g/L$, corresponding to $0.95 ppb/\sqrt{Hz}$. For nitromethane and the same minimum detectable concentration, we calculate a detection limit of $1.0 ppb/\sqrt{Hz}$. We have provided an additional analysis of the sensitivity limits of our system in Fig. 4.

Figure 5 shows spectra obtained in real-time of acetone, acetonitrile and nitromethane, as well as a spectrum from a mixture of the three. The measurements were performed at a set of pressures ranging from 0.13 *Pa* to 13.3 *Pa*, but only the 3.3 *Pa*, 6.6 *Pa* and 13.3 *Pa* spectra are displayed. The independent spectra were gathered to create a limited library, or basis set, that could be used to verify the species identification capabilities of this technique. While these species have much higher vapor pressures than explosives such as TNT or RDX, their use allows us to compare absorbers of equivalent strength at a given pressure, and allows us to demonstrate that we are able to simultaneously observe spectral features from all species in the mixture. We also note that the nitro peaks would be present in any nitro-containing explosive, that nitromethane is an explosive of relevance to national security, and that acetone is likely to be present in the explosive TATP as a residue. Also shown in Fig. 5 a set of spectra from an unknown mixture of the the three chemicals. The diagram shows spectra measured at 13.3 *Pa*, 26.6 *Pa* and 40.0 *Pa*, and illustrates the consistent behavior of the measurement technique.

The signal to noise ratio for the measurements is displayed in Fig. 4 as a function of both measured pressure (top data) and molecules interaction with the laser beam in the optical cavity (bottom data). The curves show that a signal to noise level of 2, that is, when the signal power is of equal magnitude to noise power is obtained at a cell pressure of 0.07 *Pa* (0.52 *mTorr*). The optical cavity has a resonant mode that is on average 1.2 *mm* radius and optical path length of 2 *m*. Thus the interacting volume becomes $9.0 \times 10^{-6} m^3$, and given that a mole of ideal gas a room temperature occupies $2.4 \times 10^{-2} m^3$ then the pressure data in the top curve of Fig. 4 can be displayed as shown in the bottom curve. Thus, the minimum sensitivity, expressed in moles is $3.28 \times 10^{-10} moles$. This calculation shows that the MDAL states above is an over estimate to what is achievable by the system.

In order to gather the spectra, the cavity was purged, and then evacuated using a turbomolecular pump to $\approx 10^{-4}$ *Pa*. vapor from acetone, acetonitrile and nitromethane, or the combination thereof, was allowed into the cavity by sampling the headspace above a small volume of the chemicals (less than 5 mL of each species, at room temperature and pressure). No attempt was made to concentrate the vapor). Spectra were then acquired by sweeping the laser wavelength while acquiring the output of the lock-in amplifiers. By progressively pumping out more vapor from the cavity after each spectral run, we generated the spectra shown in Fig. 5. Each spectrum is generated from the average of four sweeps, each of 152,000 separate datapoints, with scan time of 3.8 seconds per sweep.

The large tunability of our instrument allows us to observe both the symmetric and antisymmetric nitro stretches (1370 cm^{-1} and 1590 cm^{-1} respectively) as well as two strong methyl stretches of acetone (1350 cm^{-1} and 1450 cm^{-1}). The advantage of this large bandwidth is that despite the symmetric nitro stretch from nitromethane being swamped by the strong acetone absorbance, we are still able to resolve the antisymmetric stretch.

The data are replotted in Fig. 6, which shows the 13.3 Pa (100 *mTorr*) acetone, acetonitrile and nitromethane with the 40 *Pa* (300 *mTorr*) unknown sample data. The top diagram of the figure illustrates that the unknown data has key features that are similar to the pure samples but in general the spectrum is very different, and is not dominated by any one

#205644 - $15.00 USD Received 28 Jan 2014; revised 16 Mar 2014; accepted 26 Mar 2014; published 24 Apr 2014
(C) 2014 OSA

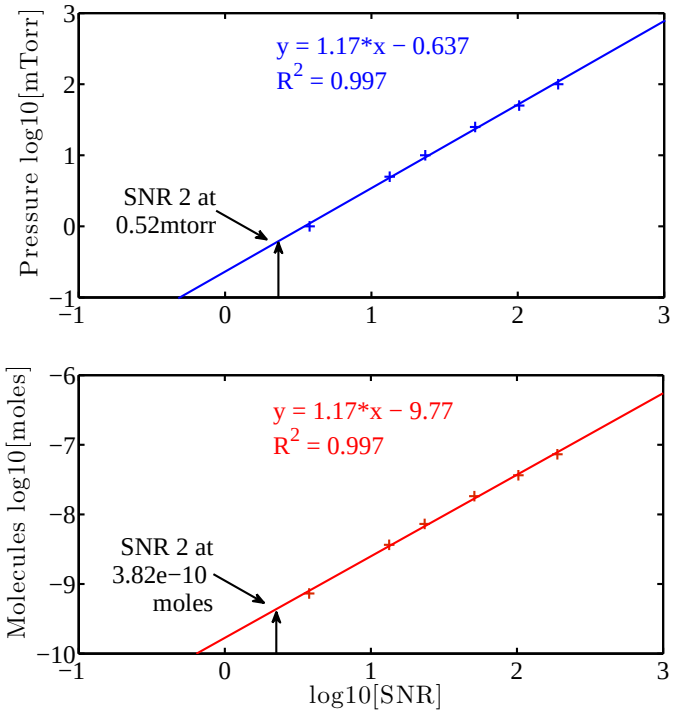

Fig. 4. A sensitivity analysis, demonstrating the detection limit as a function of approximate SNR. The SNR was determined at the peak of the acetone absorbance ($\approx 1350 cm^{-1}$): this was repeated for a series of pressures. These data are plotted in the top figure, with a linear fit. The point at which the fit shows a SNR of 2 (3 *dB*) is determined from the graph: we demonstrate a concentration of $3.28 \times 10^{-10} moles$ of acetone vapor interacting with the laser beam at this SNR. We note that the ideal gas law gives a value of 4.9×10^{-10} $moles/mTorr$ as compared to the value of 7.3×10^{-10} $moles/mTorr$ read off the graph, meaning that we are underestimating the sensitivity limit. Given the uncertainty in acetone concentration as a result of the headspace sampling method, we have not attempted to reconcile these numbers.

chemical. In fact the three chemical spectra overlap substantially. Ordinarily it would be extremely difficult to derive a quantitative estimate of the composition of the unknown spectra, but as shown in the bottom diagram an almost perfect reconstruction of the unknown spectrum can be created from a linear sum of the three spectra basis set spectra. In this case $(0.65 \times acetone) + (0.2 \times acetonitrile) + (1.6 \times nitromethane) = Unknown\ Spectra$. These data are presented to illustrate the capability of the system to produce unambiguous characterisation of an unknown sample spectrum. The possibility to gain better agreement could be achieved using better digital signal processing and better optimisation routines than a simple algebraic addition, as well as widening the measurement window by employing more laser sources.

2.3. Hypertemporal and atmospheric measurements: (1200 to 1320)cm^{-1} system.

The data presented in Sect. 2.2 used a pulsed QCL system that operated from 1316 cm^{-1} to 1613 cm^{-1} where, unfortunately, atmospheric absorption is large, as can be seen in the single pass measurements presented in Fig. 2. Although that system is perfectly adequate for pure mixtures that can be kept in isolation, it proved incapable of measuring the same samples mixed

#205644 - $15.00 USD Received 28 Jan 2014; revised 16 Mar 2014; accepted 26 Mar 2014; published 24 Apr 2014
(C) 2014 OSA

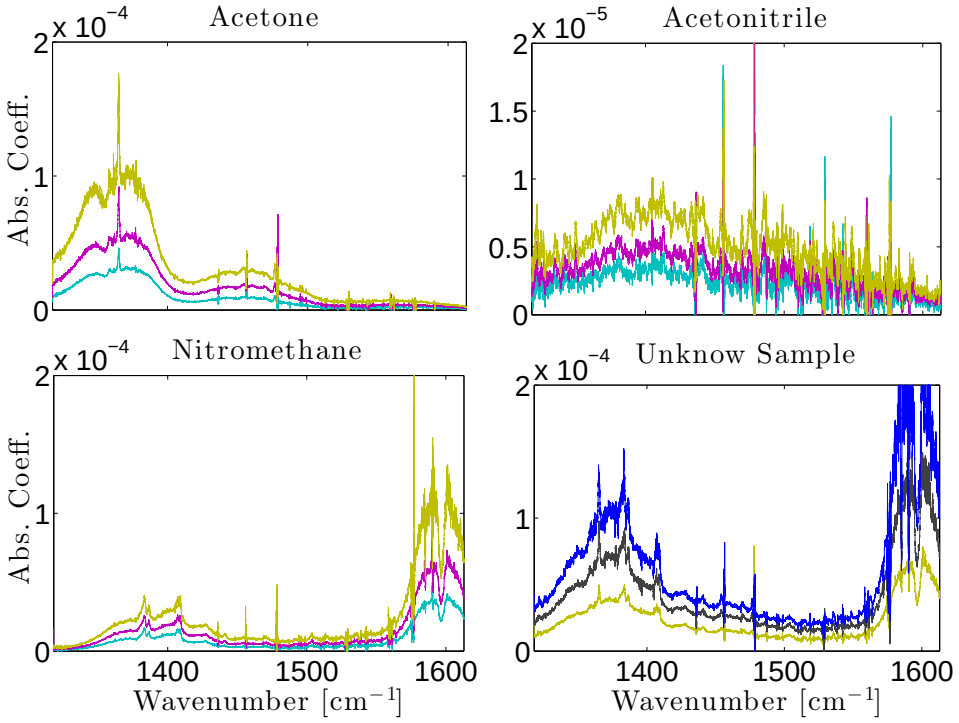

Fig. 5. The baseline subtracted spectra of the chemicals acetone, acetonitrile, nitromethane are shown at 3.33 *Pa* (25 *mTorr*) (cyan), 6.66 *Pa* (50 *mTorr*) (magenta) and 13.33 *Pa* (100 *mTorr*) (yellow) pressures. Also shown is the spectra of an unknown mixture of the three at 13.33 Pa (100 *mTorr*) (yellow), 26.7 *Pa* (200 *mTorr*) (black) and 40 *Pa* (300 *mTorr*) (blue). The subtracted background is shown in Fig. 3

with room air at from atmospheric pressure. Hence, a second system was developed that operated from 1200 cm^{-1} to 1320 cm^{-1} to make measurements in the so called "atmospheric transparency window" commonly used by thermal imaging cameras and hyperspectral IR systems. This system also allowed to apply some improvements in the experimental layout to the previous spectrometer.

This second system is similar to the first in design with several improvements. The mirror coating, the laser source, and the lock in amplifier were all changed in an attempt to improve the performance. The mirrors in this case were configured to have two 99.8% reflectance and two R_{max} mirrors in the wavelength range 1200 cm $^{-1}$ to 1320 cm^{-1}. This corresponded to a cavity decay time in the order of 700 *ns* (corresponding to an average mirror reflectance of approximately 99.7 %). All results were taken with the laser repetition rate being 150 *kHz*, with a 500 *ns* pulse width (Daylight Solutions Model ÜT-8 , the manufacturer specified pulse width is < 1 cm^{-1}). The laser was carefully aligned to the cavity such that no mode matching optics were needed: the laser coupled directly into the cavity. The result of the lower reflectance mirrors and the more efficient coupling to the cavity was an increase in transmitted power of approximately 50 times (for an incident power of approximately 2.5 *mW*, compared to the 1 μW in the previous section. This resulted in a signal from the detector (the same Kolmar detector as in section 2.2) of 2 *V cf.* 40 *mV* from the original system. Data were acquired using a Zurich Instruments HF2LI Lock-in amplifier and the results were captured directly into Matlab using the polling command and displayed in real-time. We changed lock-in amplifiers

#205644 - $15.00 USD Received 28 Jan 2014; revised 16 Mar 2014; accepted 26 Mar 2014; published 24 Apr 2014
(C) 2014 OSA

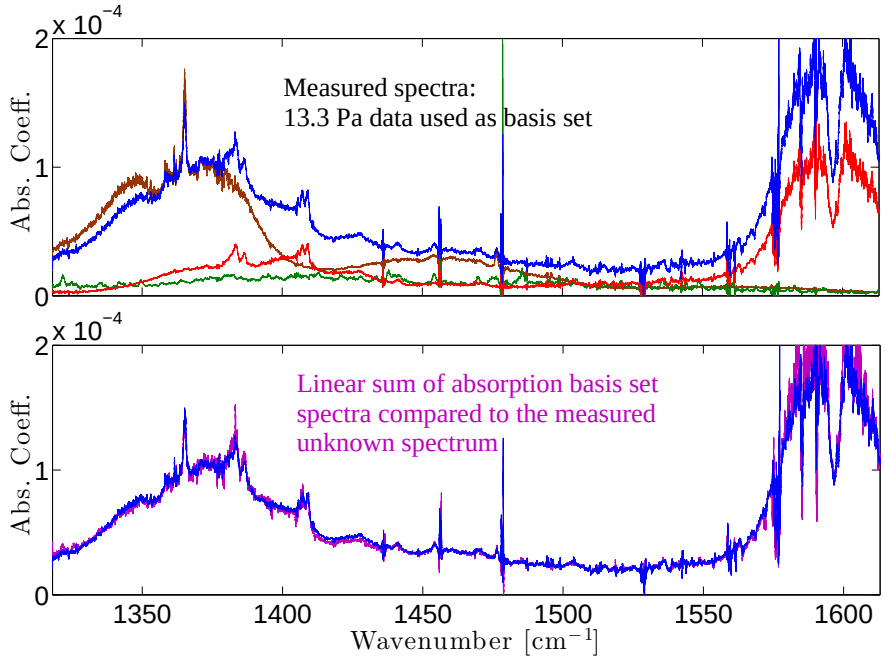

Fig. 6. The 13.3 *Pa* (100 *mTorr*) background subtracted spectra of acetone (brown), acetonitrile (green), nitromethane (red) were used to compare with the unknown sample spectrum (blue). In this case $(0.65 \times acetone) + (0.2 \times acetonitrile) + (1.6 \times aitromethane) = Unknown\ Spectra$. The subtracted background spectrum is shown in Fig. 3.

to address the spikes seen in the baseline of Figs. 2 and 3: we believe that there was a slight time delay between the two lock-in amplifiers used to calculate the power ratio. The effect of this is to generate large transients in the background files whenever there is a sharp absorbance (*e.g.* from water molecules in air) as the narrow absorbance features do not line up precisely at the output of each lock-in. Replacing the lock-in with a single model has resolved the problem, as can be seen by the smooth baseline in Fig. 7. The wavelength range was taken from the laser's display.

Using the same methodology as previously in this paper, we calculated the MDAL for this instrument: the results are shown in Fig. 7. We report a MDAL for this system of 2.6×10^{-10} $cm^{-1}/\sqrt{Hz}$. We note that this value is more than an order of magnitude better than the results for the previous system. We put this down to two main factors: the transmitted light is a factor of 50 higher than in the previous system; and the replacement of the lock-in amplifiers has eliminated the transient spikes observed in Figs. 2 and 3.

The results shown in Fig. 8 were taken with acetone vapor sampled from above a small amount of liquid acetone (approximately 5 mL of acetone in a small sample vial, at room temperature and pressure. An inlet pipe was held above the acetone, and the vacuum inside the cavity used to pull acetone vapor in. We note that this method will pull in a large amount of air along with a relatively small amount of acetone vapor. No attempt was made to preconcentrate the vapor). Fig. 8 top shows results taken when the headspace of acetone vapor was introduced into the cell at 2 *mbar* pressure (red trace) then the cell was opened to fill to atmospheric pressure (blue trace). The measurements at taken at 1000 *mbar* to maintain a slight negative pressure in the cell. As can be seen from the figure the acetone is clearly identified in both cases. The atmospheric transparency window is in fact more transparent in the range 1200

#205644 - $15.00 USD Received 28 Jan 2014; revised 16 Mar 2014; accepted 26 Mar 2014; published 24 Apr 2014
(C) 2014 OSA

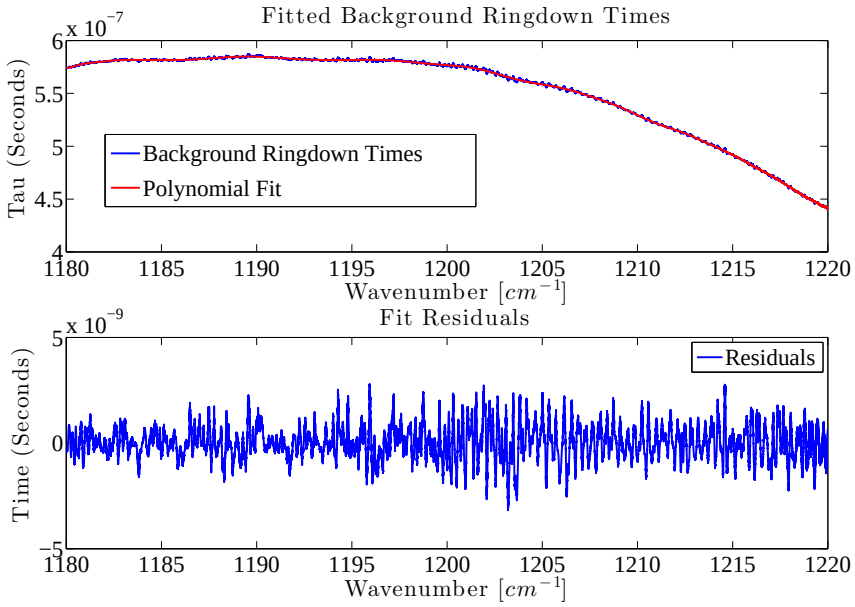

Fig. 7. Polynomial fit to background, and residuals. We note that the sharp spikes observed in Figs. 2 and 3 are no longer present.

cm^{-1} to 1320 cm^{-1} than the 1316 cm^{-1} to 1613 cm^{-1} range but the former still contains many absorbing features.

Figure 8 bottom shows results for the case where the acetone was measured remotely at distances ranging from 10 cm to 1 m in 10 cm steps. The results were taken with acetone in an open beaker sitting on the optical table with air conditioning running and no filters on the input of the cell. These results show that the acetone could be measured to at least 1 m from the cell input. In this case, 500 *mbar* of gas was allowed to enter the cell, but the range could be extended beyond 1 m for higher pressures. Also, in the case of a closed room or container, where the gasses could come to equilibrium, the system could identify contents very rapidly.

Figure 9 illustrates the real-time rapid measurement capabilities of this optical implementation. The figure shows a real-time hypertemporal scan of acetone filling the cell to a pressure of ≈ 100 *mbar*. The 4 *s* scans were taken continuously, 15 in total, and plotted immediately in Matlab. The figure clearly shows the acetone entering the cell, and could be used to identify leaks or to locate the direction of flow of a gas under investigation. Additionally, this system could be combined with a gas chromatography (GC) system to create a real-time GC-IR measurement system, which would be able to separate the headspace mixture into individual components and display them as a 3 dimensional hypertemporal cube.

In order to test the robustness of our system to vibration, we used a commercially available vibrator (Phillip Harris vibration generator, driven with a Brüel and Kjær power amplifier and a Tektronix signal generator) to excite the cavity. This caused no visible modulation of the signal on the oscilloscope, so the signal was analysed on a spectrum analyser: the results are shown in Fig. 10. No signal was observed at baseband, so the signal was viewed as intermodulation distortion around the fundamental of the waveform output of the cavity: the results are shown in Fig. 10. The largest intermodulation signal was observed using a 200 Hz excitation, resulting in sidebands at $\pm$ 400 Hz. These sidebands contain more than 70 dB less power than the fundamental, despite the large disturbance applied to the cavity. We note that it took several minutes

#205644 - $15.00 USD Received 28 Jan 2014; revised 16 Mar 2014; accepted 26 Mar 2014; published 24 Apr 2014
(C) 2014 OSA

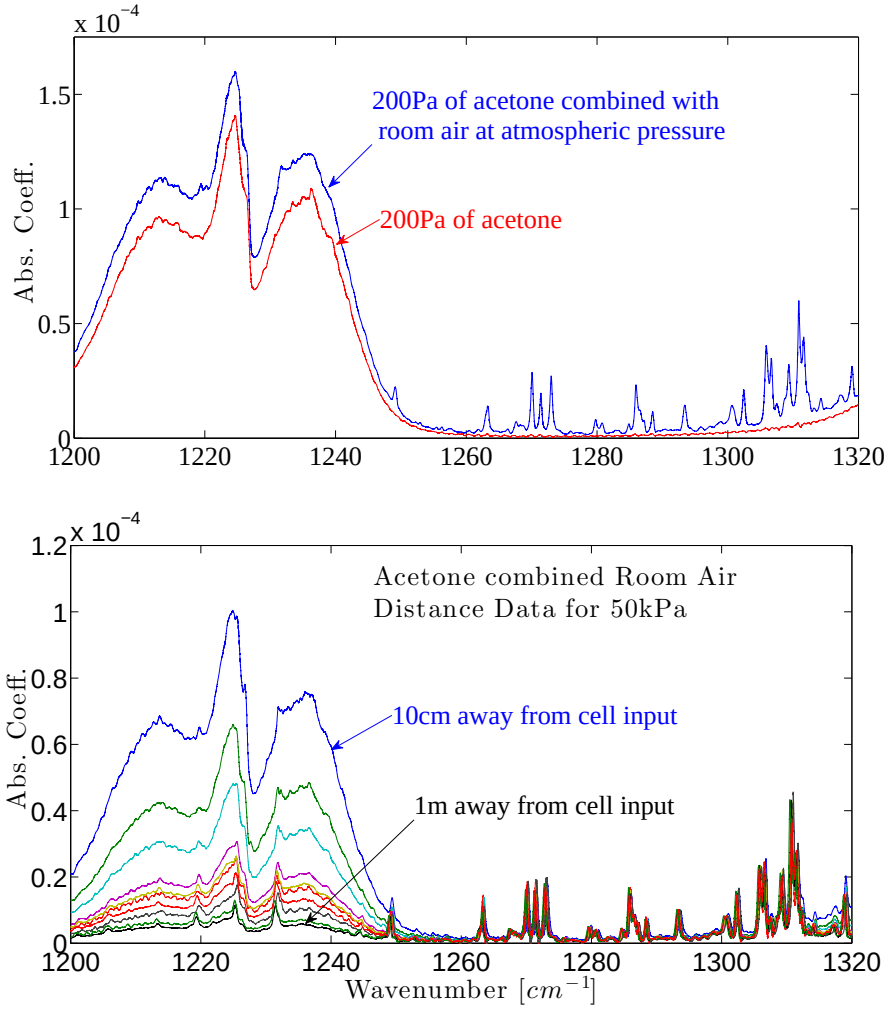

Fig. 8. Top: 200 *Pa* Acetone combined with room air added the point where the cell was at atmospheric pressure (100,000 *Pa*). Bottom: Acetone in an open vial measured in the laboratory at several distance from the cell input. Distances range from 10 cm to 1 m, in 10 cm steps. All spectra are background subtracted, with the background spectrum shown in Fig. 7

of averaging to be able to resolve the sidebands, as they are essentially the same magnitude as the noisefloor of the system.

3. Discussion

Presently the major headspace sensor being utilised by law enforcement and security agencies is the K-9. Security groups all over the world, such as the Australian K-9 Detection Unit, offer narcotics and explosive detection services to governments and non-government groups on a routine basis. The K-9 has many advantages over other methods for headspace detection but it has some major disadvantages. The most obvious being the K-9 cannot operate 24/7 or make 100% surveillance. Additionally, there are many environments that are far too hostile for a K-9

#205644 - $15.00 USD Received 28 Jan 2014; revised 16 Mar 2014; accepted 26 Mar 2014; published 24 Apr 2014
(C) 2014 OSA

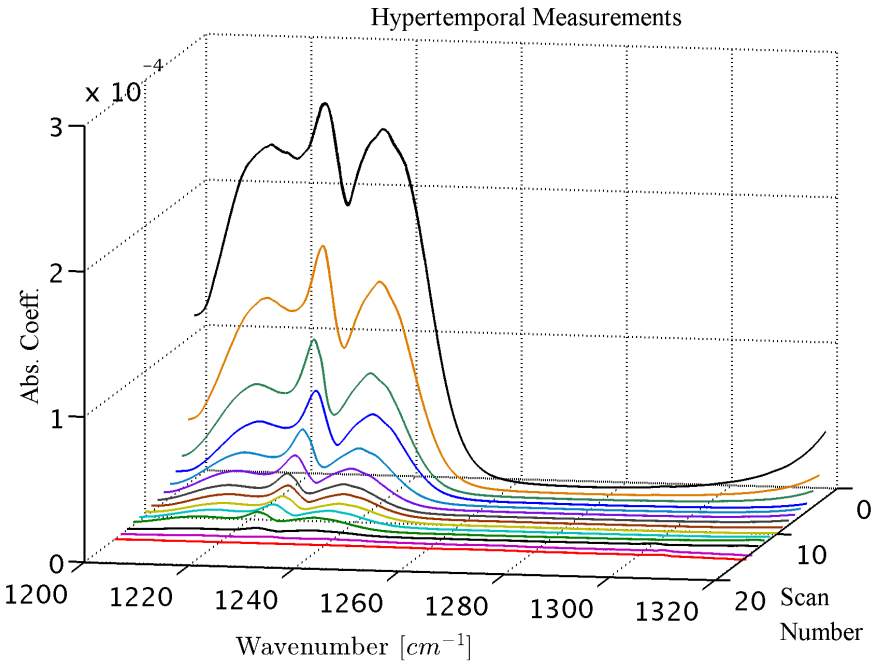

Fig. 9. Acetone in consecutive scans as the cell is filling up.

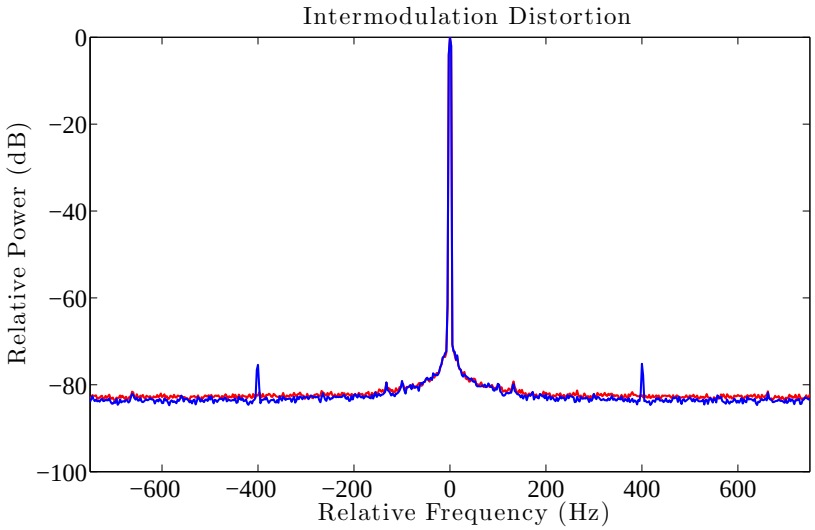

Fig. 10. Demonstration of vibration insensitivity. The cavity was excited with a Phillip Harris vibration generator: the red curve shows the cavity transmission (at 150 kHz) with no excitation, the blue curve with maximum excitation. The sidebands are more than 70 dB below the transmission peak.

#205644 - $15.00 USD Received 28 Jan 2014; revised 16 Mar 2014; accepted 26 Mar 2014; published 24 Apr 2014
(C) 2014 OSA

to enter.

Research has been performed on replicating some aspects of dogs and other biological systems to refine them into highly sensitive sensors that do not have the disadvantages of using an actual animal [21, 22]. These biologically based or inspired systems hold promise, but few are mature technologies that are ready for general use. These sensors have sensitivity and selectivity, with detection limits as low as ng/mL in solution being common [21]. The high specificity and high sensitivity of these sensors makes them attractive; however, they do not have the ability to be easily reconfigured. This high selectivity is advantageous if the explosive in question is known; it can, however, also be a disadvantage if the explosive is unknown (such as in broadscope luggage screening, or in forensic post-blast analysis). A more general spectroscopic or spectrometric method (such as mass spectrometry or absorption spectroscopy) has the ability to detect all explosives, rather than just the species for which a given sensor is designed.

Traditional CRDS systems (and essentially all of the commercially available instruments) focus on using very high reflectance (R) mirrors, with R on the order of 99.995 %, or 50 ppm transmission. This level of R leads to a ringdown time of $\approx 25\ \mu s$, or, in the frequency domain view, a corner frequency of about 6 kHz. The use of high reflectivity mirrors increases the effective pathlength of the measurement, but there is, however, a drawback to using such high reflectors: if a ringdown transient is generated, and acquired for 5-10 times the ringdown time (i.e. 125-250 μs) and the data are fit with non-linear least squares, then the throughput of the instrument is limited to less than a hundred Hz per wavelength point. If several ringdown events are averaged for each spectral datapoint, this slows the throughput even more.

Here, we demonstrate that moderate reflectance mirrors allow a sensitive measurement without sacrificing throughput. The systems presented here gather at least 50000 wavelength points per second. The systems could be set up to measure a small wavelength range many times in a given time interval, or, as shown in this paper, as a wideband single sweep. Moreover, this system could be arranged to have several mirror sets of different ringdown times to measure over different dynamic ranges, very much like a digital multimeter does in electronics. For example, increasing the R of the 1200 cm $^{-1}$ to 1320 cm^{-1} system so that the ringdown time was 7 μs rather than 0.7 μs would increase the sensitivity by a factor of 10, but would saturate more quickly and would take more time to measure, that is 5000 points per s could be taken rather than 50000 point per s. Alternatively, if the system was adjusted so that the ringdown time was 0.07 μs rather than 0.7 μs, then more points could be gathered per s but the sensitivity would decrease by a factor of 10.

Additionally, this approach leads naturally to the possibility of multiple lasers being employed simultaneously in the form of a real-time multiplexed systems. In this case, two or more lasers could be coupled through the same cell, and detected by a single photo detector if the pulse relation rates of the lasers were adjusted such that orthogonal detections of the two waves could be measured. For example, the systems presented here use a pulse repetition rate of $\approx$ 100 kHz, if a second laser used 133 kHz, then it could be measured simultaneously.

In order to test the system developed with a more widely-encountered explosive, Fig. 11 shows the spectrum of nitroglycerin spray, which is used for the prevention or relief a sudden attack of angina (chest pain) caused by heart disease. The spray works by dilating (widening) blood vessels and is carried by countless heart patients worldwide. Nitroglycerin is a component of many smokeless powders and explosives such as gelignite.

To demonstrate the instrument's ability to resolve nitro-containing molecules in the presence of atmosphere, we took spectra of 10 $mbar$ nitromethane both alone in the cell, and with room air added to atmospheric pressure: the results are shown in Fig.12. It is clear that we are able to resolve the nitromethane absorbances (in this case, the edges of the symmetric and antisymmetric nitro stretches) in the presence of water vapor from the room.

#205644 - $15.00 USD Received 28 Jan 2014; revised 16 Mar 2014; accepted 26 Mar 2014; published 24 Apr 2014
(C) 2014 OSA

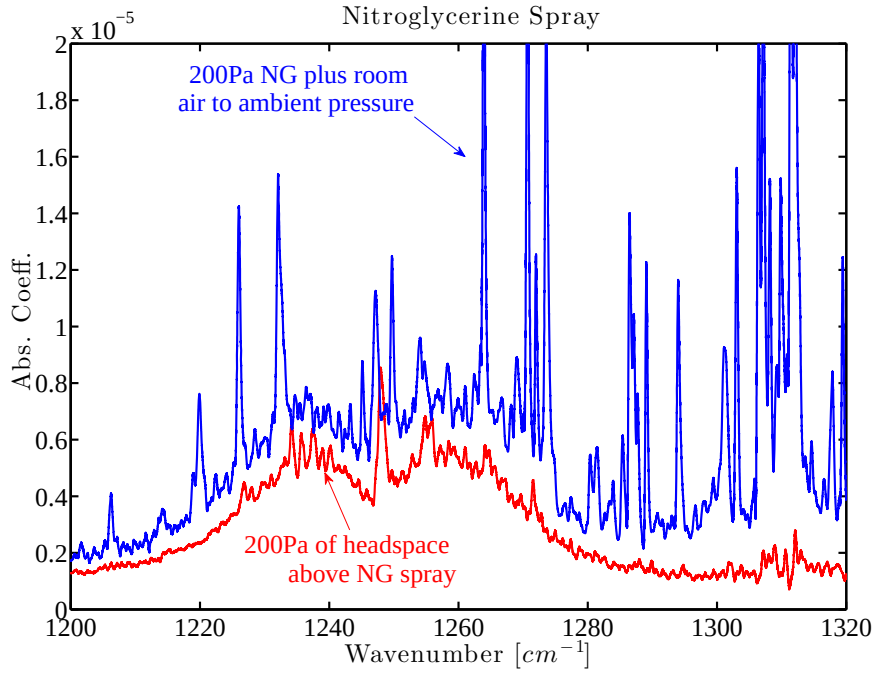

Fig. 11. 200 *Pa* (2 *mbar*) of Nitroglycerine with room air added the point where the cell was at atmospheric pressure.

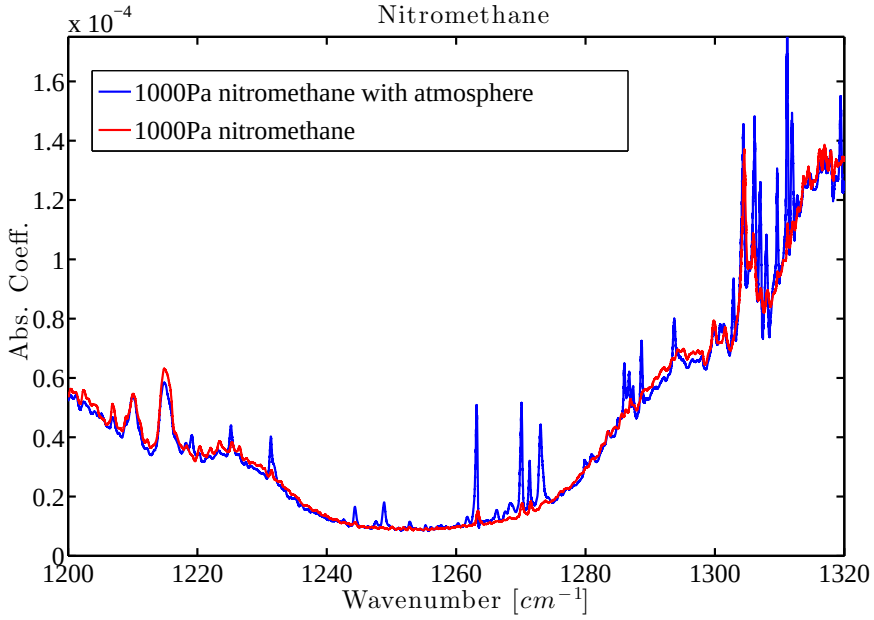

Fig. 12. 1000 *Pa* (10 *mbar*) of nitromethane with room air added to the point where the cell was at atmospheric pressure.

#205644 - $15.00 USD Received 28 Jan 2014; revised 16 Mar 2014; accepted 26 Mar 2014; published 24 Apr 2014
(C) 2014 OSA

The particular spray used here was a generic sample which contained $\approx$ 2% nitroglycerin combined with other compounds to improve the taste. The sample was measured by squirting some liquid onto a surface the measuring the headspace. The red trace in Fig. 11 shows the spectrum of 2 *mbar* of sample in the cell and is clearly different to the measured acetone, nitromethane and acetonitrile samples. The nitroglycerin shows an absorbance that is at least 10 times weaker than that of the other chemicals tested due the relatively small concentration in the spray, but is still clearly visible. The blue trace in Fig. 11 shows the 2 *mbar* sample mixed with room air, and is once again clearly visible.

4. Conclusions

We have demonstrated that cavity ringdown spectroscopy may be applied to the detection of explosives with a simple instrument that is able to rapidly scan across a large spectral bandwidth: we are able to acquire orders of magnitude more spectral datapoints than previous CRDS experiments aimed at explosives detection, and to analyse them in a fraction of the time. We are able to report noise equivalent detection limits of the order of *ppb* for acetone and nitromethane: these detection limits are gained from a very simple instrument with a very rapid analysis time.

We show that sensitive measurements can be made at atmospheric pressure and temperature as long as an adequate laser wavelength range is selected. The systems can measure the headspace of a sample located in close proximity to the unit, or up to a few meters distance from the input port. This would be ideal for measuring hostile environments such as closed rooms or shipping containers. We also show that hypertemporal data can be gathered in real-time, allowing the possibility for creating composite instruments such as gas chromatography combined with the real-time CRDS IR spectrometer to separate the headspace chemicals while measuring spectrum.

An even larger scanning range would allow for even greater selectivity: our technique allows for multiple lasers to be resonant in the cavity at the same time, provided that they have a different pulse repetition rates. We can take advantage of this to scan multiple lasers simultaneously, allowing a very large spectral bandwidth to be covered in a small amount of time. Such a system would require two lock-in amplifiers per laser, which is not viable: replacement of the lock-ins with digital signal processing [8] would allow for arbitrary scaling of the number of lasers, and thus the spectral bandwidth of the instrument.

We are presently using the instrument to analyze various explosives (both pure and in mixtures). We plan on developing a gas chromatographic front end so that we can take advantage of the physical separation of the gas chromatograph and the rapid analysis time of our technique.

Acknowledgments

We would like to thank Prof. Chris Lennard, University of Canberra, Chris Armacost and Sam Crevillo, Daylight Solutions, and Will Lohnstar, LohnStar Optics Inc., for their help during this work. This work was supported in part by the Australian Research Council, the Australian Federal Police, and ANU Connect Ventures.

#205644 - $15.00 USD Received 28 Jan 2014; revised 16 Mar 2014; accepted 26 Mar 2014; published 24 Apr 2014
(C) 2014 OSA